

AD-A129 233 ANALYSIS OF LONG BONE AND VERTEBRAL FAILURE PATTERNS
(U) FLORIDA UNIV GAINESVILLE DEPT OF PHYSIOLOGICAL
SCIENCE

1/1

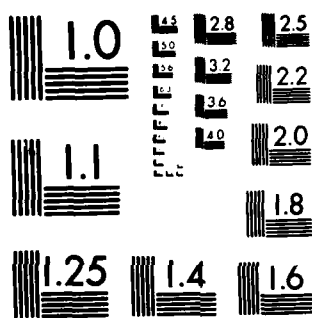
UNCLASSIFIED

AFOSR-80-0130

F/G 6/19

NL

END
DATE
FILMED
7 83
OTIC



MICROCOPY RESOLUTION TEST CHART
NATIONAL BUREAU OF STANDARDS-1963-A

(3)

AFOSR Grant Number 80-0130
Annual Technical Report
March 1983

AFOSR-80-0130

AD A129233

ANALYSIS OF LONG BONE AND VERTEBRAL
FAILURE PATTERNS

UNIVERSITY OF FLORIDA
GAINESVILLE, FL 32610

Jo Ann C. Eurell, DVM, MS, PhD

Controlling Office: USAF Office of Scientific Research/NL
Bolling Air Force Base, DC 20332

DTIC
ELECTRIC
JUN 13 1983
S A D

DTIC FILE COPY

Approved for public release;
distribution unlimited.

UNCLASSIFIED

SECURITY CLASSIFICATION OF THIS PAGE (When Data Entered)

REPORT DOCUMENTATION PAGE		READ INSTRUCTIONS BEFORE COMPLETING FORM
1. REPORT NUMBER AFOSR-TR 88-0459	2. GOVT ACCESSION NO. ADA129233	3. RECIPIENT'S CATALOG NUMBER
4. TITLE (and Subtitle) ANALYSIS OF LONG BONE AND VERTEBRAL FAILURE PATTERNS		5. TYPE OF REPORT & PERIOD COVERED Annual 1 2/20/82 through 2/19/83
		6. PERFORMING ORG. REPORT NUMBER
7. AUTHOR(s) Jo Ann C. Eurell		8. CONTRACT OR GRANT NUMBER(s) AFOSR-80-0130
9. PERFORMING ORGANIZATION NAME AND ADDRESS Dept. Physiological Sciences Box J-144, JHMH, University of Florida Gainesville, FL 32610		10. PROGRAM ELEMENT, PROJECT, TASK AREA & WORK UNIT NUMBERS 2312/A2 6/102F
11. CONTROLLING OFFICE NAME AND ADDRESS Air Force Office of Scientific Research/NL Bolling AFB, DC 20332		12. REPORT DATE March 1983
		13. NUMBER OF PAGES 23
14. MONITORING AGENCY NAME & ADDRESS (if different from Controlling Office)		15. SECURITY CLASS. (of this report) UNCLASSIFIED
		15a. DECLASSIFICATION/DOWNGRADING SCHEDULE
16. DISTRIBUTION STATEMENT (of this Report) Approved for public release; distribution unlimited.		
17. DISTRIBUTION STATEMENT (of the abstract entered in Block 20, if different from Report)		
18. SUPPLEMENTARY NOTES Material in this report was presented at the International Society for the Study of the Lumbar Spine, Toronto, Canada, June 6-10, 1982.		
19. KEY WORDS (Continue on reverse side if necessary and identify by block number) Spinal column, impaction, scanning electron microscopy, light microscopy, intervertebral discs, radiology.		
20. ABSTRACT (Continue on reverse side if necessary and identify by block number) Baboons were dropped vertically from four feet above the ground. The vertebral columns were examined with light microscopy and scanning electron microscopy. Six months post-impaction, there was damage to the vertebral end plates and beginning osteoarthritis of the facet joints. Six years post-impaction, the lesions had progressed to anterior osteophyte formation and severe osteoarthritis of the facet joints. The lesions observed in this study are thought to be related to the impaction sequence. Normal anatomy of the rhesus monkey spine was also investigated.		

UNCLASSIFIED

AFOSR Grant Number 80-0130
Annual Technical Report
March 1983

ANALYSIS OF LONG BONE AND VERTEBRAL
FAILURE PATTERNS

UNIVERSITY OF FLORIDA
GAINESVILLE, FL 32610

Jo Ann C. Eurell, DVM, MS, PhD

Controlling Office: USAF Office of Scientific Research/NL
Bolling Air Force Base, DC 20332

Accession For	
GRA&I	<input checked="" type="checkbox"/>
TAB	<input type="checkbox"/>
Unpublished	<input type="checkbox"/>
Classification	
By	
Distribution/	
Availability Codes	
Dist	Avail and/or Special
A	

AIR FORCE OFFICE OF SCIENTIFIC RESEARCH (AFSC)
NOTICE OF TRANSMITTAL TO DTIC
This technical report has been reviewed and is
approved for public release IAW AFR 13-12.
Distribution is unlimited.
MATTHEW J. KEMPER
Chief, Technical Information Division



TABLE OF CONTENTS

	Page
THE EFFECTS OF VERTICAL IMPACTION ON THE SPINAL COLUMN OF BABOONS	
INTRODUCTION	1
MATERIALS AND METHODS	1
RESULTS	2
Radiology	2
Light microscopy - anterior column.	2
Control.	2
Six month post-impaction	5
Six year post-impaction	8
Light microscopy - posterior column	9
Control.	9
Six month post-impaction	9
Six year post-impaction.	9
Scanning electron microscopy - posterior column	11
Control.	11
Six month post-impaction	11
Six year post-impaction.	11
DISCUSSION	14
Radiology	14
Light microscopy - anterior column.	14
Control.	14
Six month post-impaction	14
Six year post-impaction.	15
Light microscopy - posterior column	16
Scanning electron microscopy - posterior column	17
NORMAL ANATOMY OF THE RHESUS MONKEY VERTEBRAL COLUMN	
LITERATURE REVIEW.	18
MATERIALS AND METHODS	18
RESULTS AND DISCUSSION	18
Radiography	18
Gross dissection.	19
REFERENCES.	22
PUBLICATIONS.	22
INTERACTIONS.	23
Presentation	23
Visits to Air Force Laboratories	23
INVENTIONS AND PATENTS.	23

THE EFFECTS OF VERTICAL IMPACTION ON THE SPINAL COLUMN OF BABOONS

INTRODUCTION

The effects of vertical compressive loading on elements of the spinal column have been studied and reported during previous portions of this project.

The scanning electron microscopy of the in vivo impacted baboon spine delineated pathologic changes related to the impaction sequence. Separation of the vertebral body from the end plate was present in 6 month post-impaction animals but apparently healed by 6 years post-impaction. A region of fractured and collapsed trabeculae above the nucleus pulposus was consistently observed in impacted animals. The disc is thought to protrude into this collapsed area resulting in disc space narrowing and intervertebral joint instability. Anterior osteophytes were observed at several levels in the 6 year post-impaction animal further supporting the joint instability concept (Eurell, 1982).

The purpose of this research project was to use light microscopy to further elucidate the effects of vertical impaction on the intact spinal column of baboons. Radiology of the spines is also included.

MATERIALS AND METHODS

Vertebral columns from four baboons which were dropped vertically from four feet above the ground were examined following necropsy. The columns were shipped to Dr. Eurell from Wright-Patterson AFB. Samples received were from two baboons sacrificed six months post-impaction (G74 and G84), one baboon sacrificed six years post-impaction (E34), and one control (G30).

The vertebral columns were radiographed prior to sectioning. Anterior-posterior, lateral and oblique projections were recorded. The vertebral columns were sectioned mid-sagittally and fixed in 10% neutral buffered

formalin. Following fixation, a slab from the column was divided into smaller units and processed for scanning electron microscopy (SEM). Additional portions of the column were processed for light microscopy.

The SEM samples were dehydrated, critical point dried, and coated with gold palladium to reduce charging. Samples were scanned at 15-20 kV in a scanning electron microscope and appropriate photomicrographs were recorded.

The light microscopy samples were decalcified by the sodium citrate-formic acid method, dehydrated, and embedded in paraffin-plastic embedding material. Sections were cut on a rotary microtome and stained with hematoxylin and eosin or alcian blue-van Gieson. These sections were then observed with routine transmitted light microscopy. Appropriate photomicrographs were recorded.

RESULTS

Radiology Radiographic changes in the impacted baboons were most evident in the 6 year post-impaction animals. The most obvious radiographic change was the presence of osteophytes along the anterior border of the column (Fig. 1). The vertebral bodies were often wedge shaped in appearance indicating anterior collapse. Oblique views of the spinal column as shown in figure 2 indicated varying degrees of fusion of the facet joints.

Light microscopy - anterior column Control (G30). The vertebral bodies were composed of an exterior shell of dense cortical bone with a central core of trabecular bone. The morphology of this bone was previously described in other reports on this study. No anterior lipping, osteophytes, or fractured trabeculae were noted. The bone of the vertebral body was



Figure 1. Lateral radiograph of L₁₋₄ of a six year post-impaction animal. Note anterior osteophytes at all levels and vertebral body wedging of L₂. E18.



Figure 2. Right oblique radiograph of T₁₃-L₅ of a six year post-impaction animal. Note the partial fusion of L₁₋₂ facet joint. E18.

securely attached to the cartilaginous end plate.

The cartilaginous endplate consisted of three morphologic regions (Fig. 3). Next to the trabecular bone were areas of strongly alcian



Figure 3. Normal growth plate of control animal G30. A=annulus fibrosus, B=outer zone, non-calcified, C=outer zone, calcified, D=inner zone, E=trabecular bone. 225X, hematoxylin and eosin stain.

blue staining cartilage. These areas were scattered along the bone-cartilage interface. Above the alcian blue regions was a zone of calcified cartilage. A basophilic line separated areas of contact of the calcified cartilage with the trabecular bone of the body. Irregular basophilic regions demarcating the calcified areas were observed. These regions corresponded to the granular appearance observed with SEM. Between the intervertebral disc and the calcified cartilage

was a third zone of cartilage with flattened cells and an eosinophilic matrix. This region blended with the disc above.

Occasional regions which had scattered chondrocytes and a homogeneous eosinophilic matrix crossed the end plate perpendicular to the long axis. These corresponded to the smooth channel-like areas of SEM.

The annulus fibrosus of the intervertebral disc was intact at all observed levels. The nucleus pulposus at T₁₁₋₁₂ was chondrified. No other pathology of the intervertebral disc was observed in this animal.

Six month post-impaction (G74, G84). Fragments of trabecular bone were observed in the intervertebral discs (G84 L₁₋₂) and conversely, intervertebral disc and end plate fragments were observed in the vertebral bodies (G84 L₂₋₃) of the upper lumbar levels. Also fragments of trabecular bone were sometimes observed embedded in the cartilaginous end plates (Fig. 4).

The cartilaginous end plate was frequently fractured. The fracture line usually ran at about a 45° angle to the body axis and was located in association with the nucleus pulposus. The fracture gap was filled with alcian blue staining cartilage.

The cartilaginous end plates were usually separated from the underlying vertebral body. Three different junction patterns of the end plates and bodies were observed. The first pattern (Type I) was complete separation through the deep portion of the inner zone of the cartilage end plate with no apparent attempt at bridging (Fig. 5). This pattern seemed to occur posteriorly. The second pattern (Type II) resulted in separation through the upper portion of the inner zone (Fig. 6). Several flat



Figure 4. Fragment of trabecular bone embedded in the superior cartilaginous end plate of G84 L₃. 385X, hematoxylin and eosin stain.

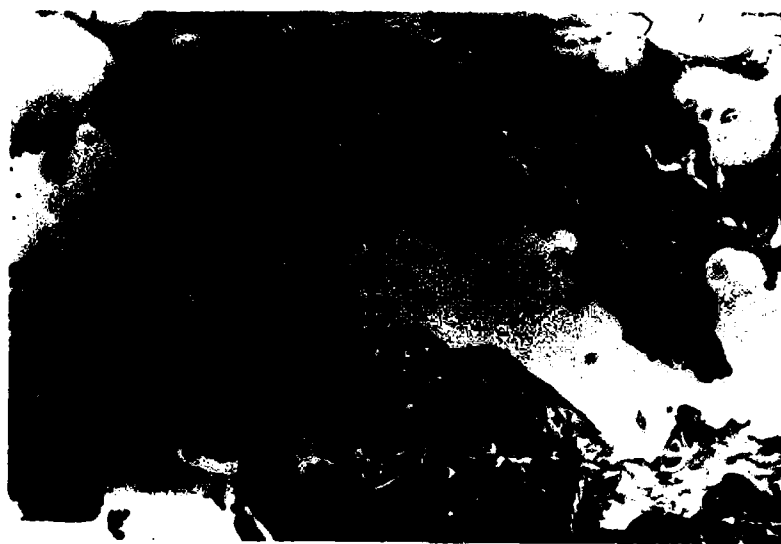


Figure 5. Type I junction of the cartilaginous end plate with the bone of the vertebral body. Note separation through the deep portion of the inner zone. Very little proliferation of chondrocytes is apparent. G74, L₁₋₂, 575X, hematoxylin and eosin stain.



Figure 6. Type II junction of the cartilaginous end plate with the bone of the vertebral body. Note separation through the upper portion of the inner zone. A=cell nest of reactive cartilage, B=proliferative region of inner zone, C=hypertrophied region of inner zone. G84, L₁₋₂, 600X, hematoxylin and eosin stain.

proliferating chondrocytes overlying a zone of hypertrophied chondrocytes were present on the vertebral side of the separation. Either necrotic cartilage devoid of cells or reactive cartilage with cell nests of 8-10 cells was present on the disc side. The third pattern (type III) was bridging between the calcified outer zone and hypertrophied region of the inner zone by columns of chondrocytes (Fig. 7). The cartilage was intensely alcian blue positive, and it corresponded to bridging struts previously reported with SEM. Both of the later types of junction seemed to occur anteriorly.



Figure 7. Type III junction of the cartilaginous end plate with the bone of the vertebral body. Columns of chondrocytes are present beneath the calcified outer zone. G74, L₃₋₄, 450X, hematoxylin and eosin stain.

Six years post-impaction (E34). The vertebral bodies of the lower thoracic and upper lumbar vertebrae had dense basophilic woven bone along their anterior margin. This reactive bone extended to form osteophytes.

The bony trabeculae around the nucleus showed evidence of fragmentation and collapse. Fragments of trabecular bone were noted in the intervertebral disc at T₁₁₋₁₂.

The cartilage in the inner zone region was disorganized (Fig. 8). The cells were arranged in clusters instead of columns and there were scattered localized areas of yellow or blue-staining fibrous tissue which separated the cell clumps.



Figure 8. End plate junction with underlying bone of 6 year post-impaction animal. Note chondrocyte clusters (arrow) separated by fibrous tissue. E34, T₁₋₂, 625X, alcian blue-van Gieson stain.

The intervertebral discs stained irregularly with increased alcian blue uptake in the anterior region.

Light microscopy - posterior column. Control (G30). No samples were obtained.

Six month post impaction (G-74, G84). Surface fibrillation and cracking of the articular cartilage was observed (Fig. 9). In some regions of the cartilage, the chondrocytes were clumped in nests of 4 to 8 cells. Alcian blue staining was diminished in the peripheral regions of the articular cartilage and around fibrillated areas.

Six years post-impaction (E34). In the central region of the articular surface, the hyaline cartilage was replaced by fibrocartilage (Fig. 10).

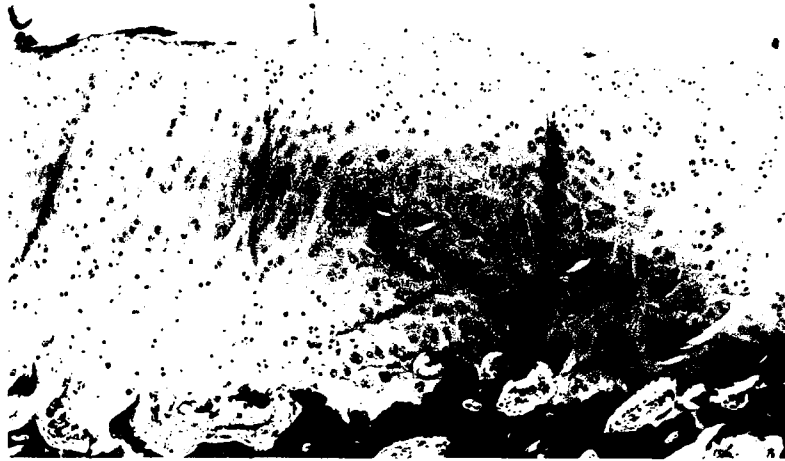


Figure 9. Articular cartilage of facet joint from a 6 month post-impaction baboon. Note fibrillation and cracks. G74, 150X, hematoxylin and eosin stain.



Figure 10. Articular cartilage of facet joint from a 6 year post-impaction baboon. The normal hyaline cartilage has converted to fibrocartilage. E34, L₅, 500X, alcian blue-van Gieson stain.

Alcian blue staining was greatly diminished. The articular surface was fibrillated.

Scanning electron microscopy - posterior column. Control (G30). The articular surface was generally smooth with a few scattered fibers (Fig. 11).



Figure 11. Articular cartilage of facet joint from a control baboon. G30, 10X.

Six month post-impaction (G74, G84). The articular surface had a central zone of fibrillation (Fig. 12). A higher magnification of this fibrillation is shown in figure 13. Peripheral to this region were several cracks in the surface of the cartilage.

Six years post-impaction (E34). The articular surface was severely fibrillated, especially in the central portion (Fig. 14). A higher magnification of the fibrillated surface is shown in figure 15.

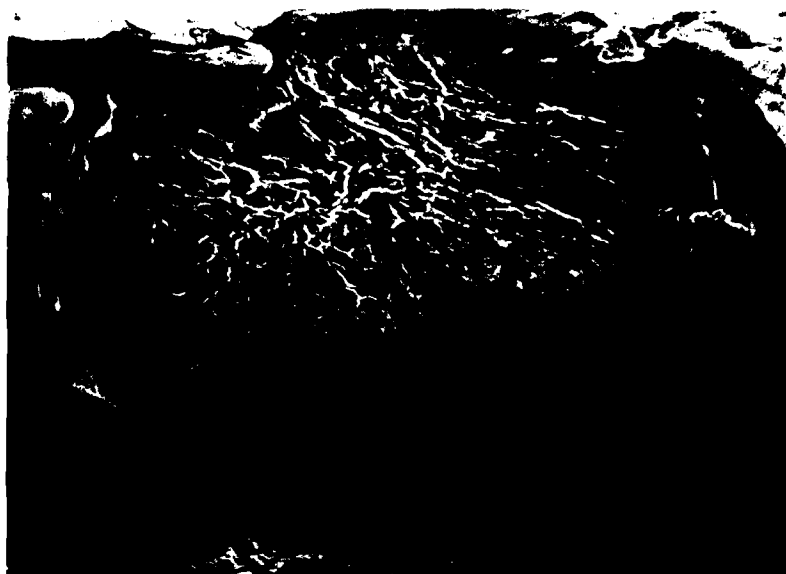


Figure 12. Articular cartilage of a facet joint from a six month post-impaction baboon. G74, 14X.



Figure 13. Higher magnification of central fibrillated region shown in figure 12. G74, 675X.

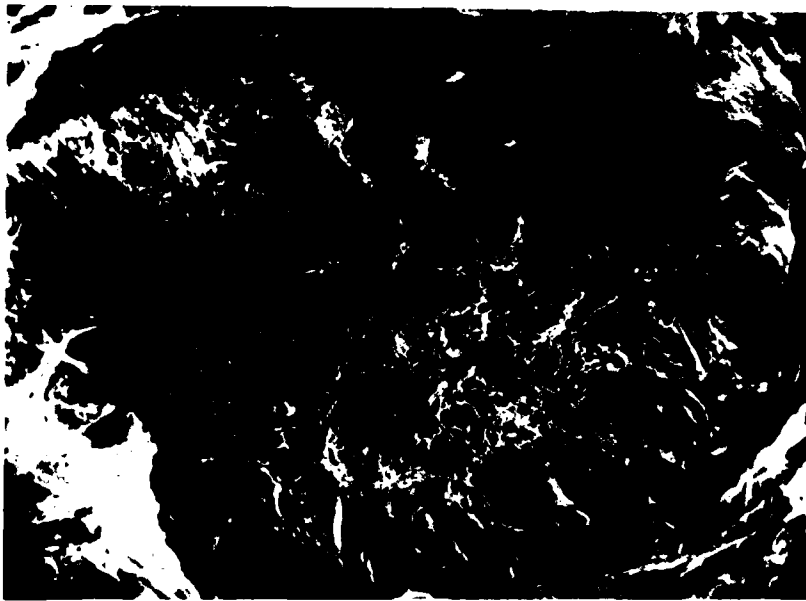


Figure 14. Articular cartilage of a facet joint from a 6 year post-impaction baboon. E34, L₆ anterior, 10X.



Figure 15. Higher magnification of fibrillated region shown in figure 14. E34, 325X.

DISCUSSION

Radiology. The radiographic changes visible in the six year post-impaction animal indicated the presence of degenerative spondylosis. Changes were not present in the six month post-impaction animals because degeneration of the spine was not progressive enough to be evident radiographically.

Light microscopy - anterior column. Control (G30). This animal was within normal limits except for the pathology previously noted in the intervertebral disc at T₁₁₋₁₂.

The morphologic regions of the cartilaginous end zone compare to those described in mice by Higuchi, et al (1982). The inner zone is narrowed as if the vertebrae of this animal were approaching skeletal maturity.

The regions of the plate with homogeneous matrix and scattered chondrocytes are probably either scarring from vessel pathways of early development or scarring from the embryonic notochord which passes through this area.

Six months post-impaction (G74,G84). Displaced fragments of trabecular bone, cartilaginous end plate, or disc material were probably the results of the impaction sequence. The impaction sequence was also most likely responsible for the fractures and separations of the cartilaginous end plates.

The separation of the end plates occurred between two regions of calcified tissue. This location would be expected based on the "sandwich" structure of the interface. The uncalcified tissue would be expected to yield before the calcified cartilage or bone.

The configuration of the type I and II junctions may be related to the path of the separation. If the disruption courses through the deep hypertrophied region of the inner zone, the cells on the vertebral side

of the gap may be beyond the point where they have the potential to divide. The cartilage on the disc-side of the gap is removed from its nutritional source and is degenerating. Therefore, the separation remains open. If the separation occurs in the upper proliferating region, then the cells may still be able to divide and proliferate to eventually bridge the gap.

The gap may also remain open because of fluid which collects in the space and somehow slows rejoining of the interfaces.

The type III junction represents either a rejoining of the separated zones by cartilage proliferation or an area which was not damaged by the original impact. Further studies of immediate post-impaction animals is indicated to elucidate the nature of this junction.

An interesting sidelight to these junction patterns is the question of nutrition to the end plate region. Töndury (1958) stated that the vertebral body and cartilage plate receive their blood from the same sources while a separate vascular circulation supplies the disc. Francois and Dhem (1974) showed capillaries from the vertebral body penetrating the calcified cartilage to contact the uncalcified cartilage above.

Our study would support two blood supplies to the end plate based on the cartilaginous response to separation. The cartilage on the body side of the separation remains viable while the inner zone portion on the disc side degenerates. The outer zone on the disc side of the separation remains healthy however, indicating that it still has a viable nutrient supply.

Six year post-impaction, (E34). The initial impact sequence resulted in fragmented trabeculae above the nucleus pulposus which were previously reported with SEM (Eurell, 1982). Evidence of these collapsed trabeculae

were still present in the six year post-impaction vertebrae when viewed with light microscopy.

The separation of the end plate from the underlying vertebral body observed in the six month post-impaction animals is not present in the six year post-impaction animals, and therefore it may heal with time. The shape of the endplates is influenced by the progressive ossification of the vertebral body (Donisch and Trapp, 1971). The initial damage to the plate may result in a defect in endochondral ossification. The disorganization of the cartilage at the junction region is probably a combination of changes related to growth plate closure and cartilage disruption due to the impaction sequence. The combination of damage to the end zone trabeculae induced by the incompressible nucleus pulposus and the possible disruption of bone growth due to the end plate damage may result overall in a very irregular vertebral end zone. This irregular end zone may contribute to some degree of joint instability.

Another contributing factor to joint instability is vertical fractures in the end plate. These fractures create a pathway for the escape of disc material and subsequent collapse of the disc space. The resultant joint instability then leads to formation of anterior osteophytes in an attempt to stabilize the joint.

The irregular staining of the intervertebral disc further supports the overall degeneration of the intervertebral joint. The annulus fibrosus is apparently attempting to respond to the joint instability by producing more mucopolysaccharides and building up more fibrocartilage.

Light microscopy-posterior cartilage. The surface fibrillation and cracking of the facet joint articular cartilage along with clumping of the chondrocytes and diminished alcian blue staining is indicative of cartilage degeneration.

The changes seem to increase in severity with time as evidenced by the six year post-impaction sample in which more severe osteoarthrosis is present. The degenerative changes observed in the posterior articulations of the vertebral column are probably resultant of the preceeding intervertebral joint instability as proposed by Vernon-Roberts (1980).

Scanning electron microscopy - posterior column. The surface of the articular cartilage of the control animal was relatively smooth compared to the impacted animal joint surfaces. Fibrillation was evident on the articular surfaces of the joints from six month post-impaction animals and it had progressed to a more extensive, severe lesion of the cartilage in the six year post-impaction group. The fibrillation is indicative of osteoarthrosis and is thought to be related to the impaction process. The SEM findings also support the light microscopy presented above.

NORMAL ANATOMY OF THE RHESUS MONKEY VERTEBRAL COLUMN

LITERATURE REVIEW

The vertebral formula for the rhesus monkey is $C_7T_{12}L_7S_3Cd_{\pm 20}$.

Sherrington (1892) and Schultz (1930) have reported individual variations in the formula at different levels of the column. An excellent discussion of the specific gross anatomy of the rhesus monkey vertebral column has been published by Sullivan (1969). It will not be repeated here.

Stillwell (1956) discussed the nerve supply to the vertebral column and its associated structures. Of particular interest to this study is the innervation of the facet joints. The dorsal ramus of the spinal nerve arises just distal to the spinal ganglion. The ramus divides into several branches. Major branches from each spinal nerve supply two successive articulations, and therefore, each joint has bisegmental innervation. A single lumbar spinal nerve supplies an articulation near its emergence and another joint one vertebra caudally.

MATERIALS AND METHODS

Five rhesus monkey vertebral columns were collected and frozen. Anterior-posterior, lateral and oblique radiographs were taken. The spines were fixed in ten per cent neutral buffered formalin.

Following fixation, the nerve supply to the posterior facet joints was dissected at several lumbar levels. Attempts to dissect musculature were unsuccessful because freezing made the tissue too friable.

The vertebral column was slabbed with a meat saw into smaller sections for scanning electron microscopy and light microscopy. The samples are currently being processed for each of those techniques.

RESULTS AND DISCUSSION

Radiography. Radiographs of the lumbar region of the normal rhesus

monkey spine are shown in figures 16-19. The vertebral bodies were



Figure 16. A-P radiograph of T₁₁-L₇, normal rhesus monkey.

square to rectangular in shape and symmetrical. The disc spaces and vertebral processes were of normal conformation. No osteophytes were present. One posterior facet joint (T₁₂-L₁) of one animal (RM5) was fused; the rest were within normal limits.

Gross dissection. The distribution of the dorsal and ventral rami of the spinal nerves as determined by dissection is shown in figure 20. The dorsal ramus of the spinal nerve branches to supply epaxial muscles in the area as well as the posterior facet joint at the level of the emergence of the spinal nerve and the facet joint immediately caudal. This innervation concurs with the findings of Stilwell (1956).

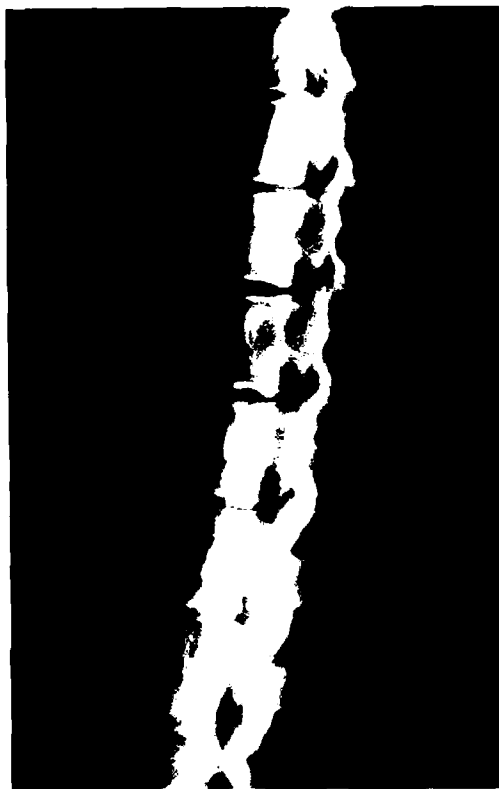


Figure 17. Lateral radiograph of T₁₂-L₇, normal rhesus monkey.



Figure 18. Right oblique of T₁₁-L₇, normal rhesus monkey.



Figure 19. Left oblique of T₁₁-L₇, normal rhesus monkey.

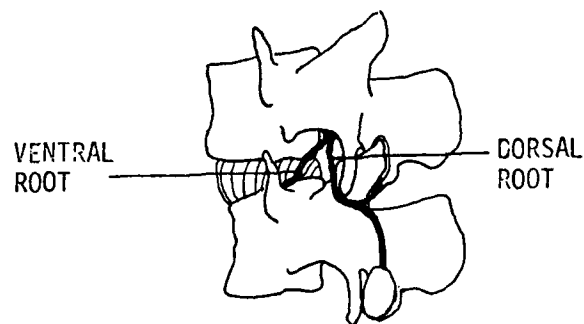


Figure 20. Sketch of the innervation to the posterior facet of the rhesus monkey.

REFERENCES

- Donisch, E.W. and W. Trapp, 1971. The cartilage endplates of the human vertebral column (some considerations of postnatal development). *Anat. Rec.* 169: 705-716.
- Eurell, J.C., 1982. Analysis of long bone and vertebral failure patterns. Annual technical report, AFOSR Grant Number 80-0130, March 1982.
- Francois, R.J. and A. Dhem, 1974. Microradiographic study of the normal human vertebral body. *Acta anat.* 89: 251-265.
- Higuchi, M., K. Kaneda, and K. Abe, 1982. Postnatal histogenesis of the cartilage plate of the spinal column. Electron microscopic observations. *Spine* 7: 89-96.
- Schultz, A.H., 1930. The skeleton of the trunk and limbs of higher primates. *Human Biol.* 2: 303.
- Sherrington, C.S., 1892. Notes on the arrangement of some motor fibers in the lumbosacral plexus. *Jour. Physiol.* 13: 621.
- Stilwell, D.L., 1956. The nerve supply of the vertebral column and its associated structures in the monkey. *Anat. Rec.* 125: 139-169.
- Sullivan, W.E., 1969. Skeleton and joints in Hartman, C.G. and W.L. Straus, Jr. (eds) *The Anatomy of the Rhesus Monkey*, Hafner Publ. Co., pp. 43-84.
- Töndury, G., 1958. *Entwicklungsgeschichte und fehlbildungen der wirbelsäule*. Hippokrates Verlag, p. 71.
- Vernon-Roberts, B., 1980. The pathology and interrelation of intervertebral disc lesions, osteoarthritis of the apophyseal joints, lumbar spondylosis and low back pain in Jayson, M.I.V. (ed) *The Lumbar Spine and Back Pain*, Pitman Medical, pp. 83-114.

PUBLICATIONS

- Eurell, J.C. and L.E. Kazarian, The scanning electron microscopy of compressed vertebral bodies. *Spine* 7(2): 123-128, 1982.
- Eurell, J.A. and L.E. Kazarian, The quantitative histochemistry of rat lumbar vertebrae following spaceflight. *The Physiologist*, in press for March-April 1983.
- Eurell, J.C., L.E. Kazarian, P. Gordon, and W. Blakeney, The scanning electron microscopy of compressed spinal units. Submitted to *Anatomica Clinica*, September 1982.

INTERACTIONS

Presentation

Eurell, J. and L. Kazarian. The scanning electron microscopy of the vertebral column from baboons following vertical impaction, June 6-10, 1982, International Society for the Study of the Lumbar Spine, Toronto, Canada.

Visits to Air Force Laboratories

June 21-13, 1982 to Wright Patterson AFB, AFAMRL/BBD.

December 19-21, 1982 to Wright Patterson AFB, AFAMRL/BBD.

INVENTIONS AND PATENTS

None.

DATE
ILME